

SELF-CONDITIONED DIFFUSION MODEL FOR CONSISTENT HUMAN IMAGE AND VIDEO SYNTHESIS

Anonymous authors

Paper under double-blind review

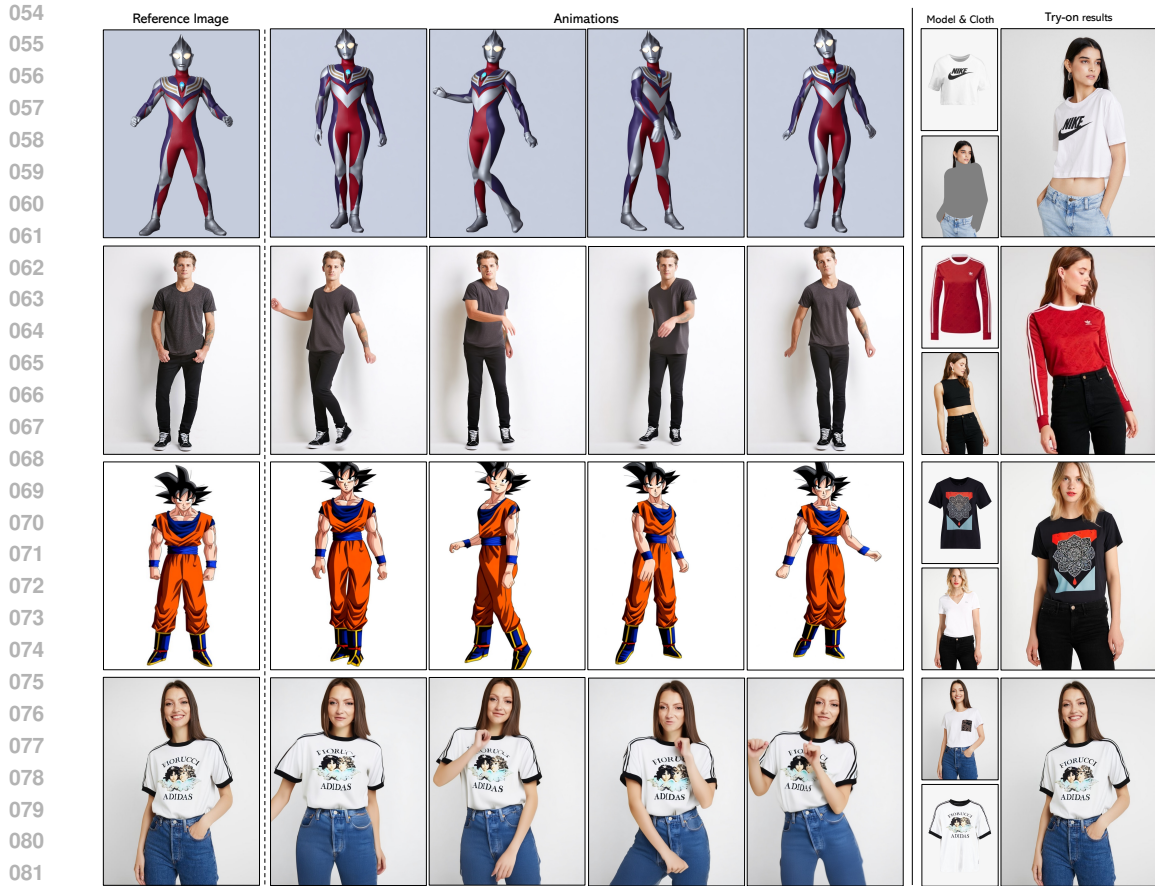
ABSTRACT

Consistent human-centric image and video synthesis aims to generate images or videos with new poses while preserving appearance consistency with a given reference image, which is crucial for low-cost visual content creation. Recent advancements based on diffusion models typically rely on separate networks for reference appearance feature extraction and target visual generation, leading to inconsistent domain gaps between references and targets. In this paper, we frame the task as a spatially-conditioned inpainting problem, where the target image is inpainted to maintain appearance consistency with the reference. This approach enables the reference features to guide the generation of pose-compliant targets within a unified denoising network, thereby mitigating domain gaps. Additionally, to better maintain the reference appearance information, we impose a causal feature interaction framework, in which reference features can only query from themselves, while target features can query appearance information from both the reference and the target. To further enhance computational efficiency and flexibility, in practical implementation, we decompose the spatially-conditioned generation process into two stages: reference appearance extraction and conditioned target generation. Both stages share a single denoising network, with interactions restricted to self-attention layers. This proposed method ensures flexible control over the appearance of generated human images and videos. By fine-tuning existing base diffusion models on human video data, our method demonstrates strong generalization to unseen human identities and poses without requiring additional per-instance fine-tuning. Experimental results validate the effectiveness of our approach, showing competitive performance compared to existing methods for consistent human image and video synthesis.

1 INTRODUCTION

The field of human-centric image and video generation focuses on creating novel images or videos that conform to specified poses while maintaining appearance consistency with a reference image. Recent advancements [Hu et al. \(2023\)](#); [Xu et al. \(2023\)](#); [Wang et al. \(2023\)](#); [Chang et al. \(2023\)](#) have shown promising human image customizing or animating results, and have potential applications in entertainment, e-commerce, and education. The primary challenge lies in preserving appearance consistency, especially fine details, between the reference image and the generated outputs.

Traditional approaches [Chan et al. \(2019\)](#); [Ren et al. \(2020\)](#); [Siarohin et al. \(2019\)](#); [Zhang et al. \(2022\)](#); [Zhao & Zhang \(2022\)](#); [Ren et al. \(2022\)](#); [Han et al. \(2018\)](#); [Yang et al. \(2020\)](#); [Choi et al. \(2021\)](#); [Ge et al. \(2021\)](#); [Xie et al. \(2023\)](#) typically rely on estimating correspondence between the reference and target images, followed by the use of warping modules to deform the reference image into the target pose. The final results are generated using conditional GANs. However, these methods often struggle to preserve fine details, resulting in artifacts such as low resolution, distortion, loss of detail, and inconsistent appearance, limiting their practical applicability. Recently, diffusion-based models [Ho et al. \(2020\)](#); [Saharia et al. \(2022\)](#); [Rombach et al. \(2022\)](#); [Dhariwal & Nichol \(2021\)](#); [Peebles & Xie \(2023\)](#); [Guo et al. \(2023\)](#); [Blattmann et al. \(2023a\)](#) have shown significant promise in generating photorealistic images and videos. By leveraging these powerful generative models, recent studies [Bhunia et al. \(2023\)](#); [Karras et al. \(2023\)](#); [Wang et al. \(2023\)](#) have produced higher-quality human images and videos compared to GAN-based methods. These models typically



083 Figure 1: We propose self-conditioned diffusion (SCD) for consistent human image and video synthesis. Left part: our method can generate content-consistent human videos given a reference human
 084 image and target poses. Right part: our method can also be applied to visual try-on to maintain the
 085 appearance details of the garment.
 086

087

088 inject reference image features, extracted by the CLIP image encoder [Radford et al. \(2021\)](#); [Karras et al. \(2023\)](#), into the denoising network or concatenate the reference image with noise along the
 089 input channel. However, they still face challenges in preserving fine-grained details: CLIP excels at
 090 embedding semantic-level information but struggles to capture discriminative representations neces-
 091 sary to preserve appearance [Chen et al. \(2023\)](#). Similarly, channel concatenation tends to prioritize
 092 spatial layout over identity and appearance consistency.
 093

094 Recent studies [Cao et al. \(2023\)](#); [Khachatryan et al. \(2023\)](#); [Zhang et al. \(2023\)](#) have demonstrated
 095 that pretrained text-to-image diffusion models can generate content-consistent images and videos in
 096 a zero-shot manner by manipulating the self-attention layers within the denoising network. How-
 097 ever, these zero-shot methods often suffer from unstable generation results and struggle to maintain
 098 fine-grained details. To address these challenges, [AnimateAnyone Hu et al. \(2023\)](#) and [MagicAn-
 099 imate Xu et al. \(2023\)](#) introduce an additional trainable copy of the denoising U-Net, known as
 100 Reference-Net, to extract appearance features and inject them using the denoising U-Net’s self-
 101 attention layers during the denoising process. While this approach has set new benchmarks in con-
 102 sistent human image and video generation, these methods typically require substantial resources to
 103 train such a large Reference Network. Furthermore, an inconsistent domain gap remains between
 104 the reference features extracted by the Reference-Net and the target features in the denoising U-Net,
 105 which limits their ability to fully preserve appearance consistency.

106 In this work, we propose the self-conditioned diffusion (SCD) model for high-quality human-centric
 107 image and video synthesis, with a focus on preserving appearance consistency. Unlike previous
 methods that rely on additional networks to extract reference appearance information, SCD lever-

ages the denoising U-Net itself to directly condition the reference image spatially. This approach ensures that both reference and target features reside within the same feature manifold, enabling better preservation of appearance details compared to Reference-Net-based methods [Xu et al. \(2023\)](#); [Chang et al. \(2023\)](#); [Hu et al. \(2023\)](#). Our approach is inspired by the capability of the pretrained Stable Diffusion model [Rombach et al. \(2022\)](#) to perform zero-shot inpainting and generate harmonious, content-consistent results. By fine-tuning this base model and applying spatial conditioning to the reference image (via spatial concatenation), we effectively preserve both texture and appearance details. To further enhance appearance preservation, we introduce a causal interaction framework within the denoising U-Net, where reference features are restricted to querying from themselves, while target features can query from both reference and target features. This framework ensures that the reference image’s fine-grained appearance details are retained throughout the generation process. Furthermore, the spatial conditioning process is decomposed into two sub-processes to allow for a more flexible and efficient generation in the practical implementation: 1) the reference image is passed through the denoising network to extract appearance features, and 2) the target image is then generated by conditioning on these intermediate reference features. As illustrated in Fig. 1, our method synthesizes human images or videos that faithfully maintain the reference appearance while conforming to specified target poses.

Our contributions can be summarized as follows: **1)** We propose a spatial conditioning strategy for reference-based human generation, framing the task as an inpainting problem. The target human image is inpainted under the spatially conditioned reference image, ensuring appearance consistency. **2)** A causal feature interaction mechanism is incorporated within the denoising U-Net to ensure fine-grained preservation of reference appearance details, which allows target features to query from both the reference and target features, while reference features query only from themselves. **3)** We further separate the causal feature interaction framework into two sub-processes: reference feature extraction and subsequent conditioned generation. This design enhances the flexibility, effectiveness, and efficiency of the generation process. **4)** Experimental results demonstrate the effectiveness and competitiveness of our method in generating consistent human-centric images and videos compared to existing methods.

2 RELATED WORKS

2.1 DIFFUSION MODEL FOR IMAGEN AND VIDEO GENERATION

Diffusion models [Sohl-Dickstein et al. \(2015\)](#); [Ho et al. \(2020\)](#); [Song & Ermon \(2019\)](#); [Song et al. \(2020b\)](#) have significantly advanced visual content generation, achieving superior results and leading the field. In image generation, various diffusion-based methods such as GLIDE [Nichol et al. \(2021\)](#), LDM [Rombach et al. \(2022\)](#), DALLE-2 [Ramesh et al. \(2022\)](#), Imagen [Saharia et al. \(2022\)](#), and DiT [Peebles & Xie \(2023\)](#) have been developed to synthesize photorealistic images that comply with additional class labels or textual descriptions. To enable more controllable synthesis with diffusion models under spatial controls like edge, pose, depth, and segmentation maps, research works such as ControlNet [Zhang et al. \(2023\)](#); [Zhao et al. \(2024\)](#) and T2i-Adapter [Mou et al. \(2024\)](#) incorporate additional controls into pretrained diffusion models by integrating trainable networks. Furthermore, these pretrained diffusion models are also employed for image editing. Dreambooth [Ruiz et al. \(2023\)](#) and Textual Inversion [Gal et al. \(2022\)](#) fine-tune the diffusion model parameters and optimize the textual embedding, respectively, to perform subject-driven image editing. Additionally, some tuning-free methods [Meng et al. \(2021\)](#); [Hertz et al. \(2022\)](#); [Tumanyan et al. \(2023\)](#); [Cao et al. \(2023\)](#) control the denoising process to perform editing without any additional fine-tuning. Building on the success of diffusion models in the image generation domain, researchers have also extended these models for spatiotemporal modeling in video generation [Ho et al. \(2022b;a\)](#); [Singer et al. \(2022\)](#); [Hong et al. \(2022\)](#); [Blattmann et al. \(2023b\)](#); [Khachatryan et al. \(2023\)](#); [Guo et al. \(2023\)](#); [Blattmann et al. \(2023a\)](#). These models have also been explored for video editing [Wu et al. \(2023\)](#); [Liu et al. \(2023\)](#); [Geyer et al. \(2023\)](#); [Qi et al. \(2023\)](#); [Ceylan et al. \(2023\)](#); [Yang et al. \(2023b\)](#), achieving considerable success in terms of visual quality and consistency of the edited videos. Building on these successful visual generation models, we explore consistent human image and video synthesis.

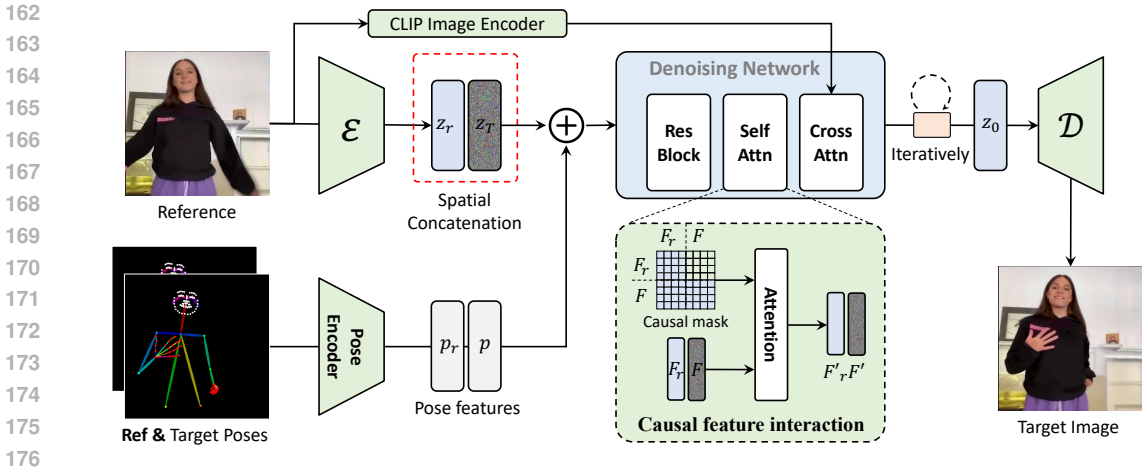


Figure 2: Overview of the self-conditioned diffusion model. Our framework achieves consistent human image and video synthesis by inpainting the desired image under the spatially conditioned reference human image using only the denoising network. A causal feature interaction and reference pose information injection are introduced to further ensure the content consistency between the generated and reference images.

2.2 CONSISTENT HUMAN IMAGE AND VIDEO SYNTHESIS WITH DIFFUSION MODELS

Employing diffusion models for synthesizing human-centric visual content has been extensively studied recently, encompassing tasks such as pose transfer [Bhunia et al. \(2023\)](#), human image animation [Karras et al. \(2023\)](#); [Hu et al. \(2023\)](#); [Xu et al. \(2023\)](#), and visual try-on [Chen et al. \(2023\)](#); [Huang et al. \(2023\)](#); [Yang et al. \(2023a\)](#). The primary challenge lies in preserving the texture details and identity of the reference human image. Initial attempts [Yang et al. \(2023a\)](#); [Huang et al. \(2023\)](#); [Chen et al. \(2023\)](#); [Wang et al. \(2023\)](#) aimed to synthesize images with textures similar to the reference image by encoding the reference image using the CLIP image encoder [Radford et al. \(2021\)](#) or the DINO image encoder [Caron et al. \(2021\)](#). However, these methods often struggle to achieve highly detailed texture consistency between the synthesized and reference images. Further research [Gou et al. \(2023\)](#); [Bhunia et al. \(2023\)](#); [Kim et al. \(2023\)](#); [Zhu et al. \(2023\)](#) has explored explicit image warping with flow or implicit warping using attention mechanisms to achieve more consistent edited results. More recently, researchers [Hu et al. \(2023\)](#); [Xu et al. \(2023\)](#); [Zhu et al. \(2024\)](#) have designed Reference-Net-based frameworks that utilize a copy of the denoising U-Net to extract intermediate features and inject them into the denoising U-Net using a reference attention mechanism, thereby achieving much higher consistency in preserving identity and texture details. Meanwhile, this Reference-Net framework has also been adapted to visual try-on [Xu et al. \(2024\)](#); [Choi et al. \(2024\)](#) to achieve better try-on results. In this work, we design a unified diffusion-based framework for human-centric visual content generation and explore self-consistency in the denoising U-Net to achieve appearance consistency between the reference and target images.

3 METHOD

3.1 SPATIALLY-CONDITIONED DIFFUSION FOR CONSISTENT HUMAN GENERATION

Given a reference human image I_r , our objective is to generate new images or videos that preserve the identity of the person in the reference image while adhering to specified target poses. Achieving this objective involves several key challenges: **1)** Maintaining content consistency, including the background, human details, and identity, between the reference image and the generated outputs; **2)** Ensuring that the generated images or videos align accurately with the provided target poses. To address these challenges simultaneously, we propose a self-conditioned diffusion-based model. This model harnesses the denoising network for appearance feature extraction and employs self-conditioning to ensure high-quality, consistent generation of human images and videos.

Content Consistency through Spatial Conditioning. Our approach is inspired by the observation that pretrained text-to-image diffusion models, such as Stable Diffusion [Rombach et al. \(2022\)](#), are capable of performing zero-shot inpainting, seamlessly filling masked regions with content that is consistent with the unmasked areas. Additionally, these models can extend a given reference image to a larger one, a process known as outpainting (as shown in Fig. 3(a)). This behavior suggests that pretrained diffusion models inherently generate complete and harmonious images rather than disjoint or fragmented ones. Leveraging this, the added spatial conditioning facilitates the generation of images with a high degree of content consistency.

Motivated by these observations, we propose a spatially-conditioned diffusion model designed for the consistent generation of human images, leveraging large pretrained diffusion models such as Stable Diffusion [Rombach et al. \(2022\)](#). During the training phase, we concatenate the reference image latents with the noisy target image latents along the spatial axis, inputting them into the denoising network. The denoising network predicts the added noise (or other relevant predictions), while the noisy region associated with the target image is cropped to calculate the diffusion loss, as specified in Eq. 4 in the Appendix. As the generation process is conditioned on the reference features extracted by the denoising network itself, we refer to it as self-conditioned diffusion (SCD).

This straightforward spatial conditioning strategy ensures that both reference and target features occupy the same feature domain manifold, thereby enhancing the transfer of appearance details from the reference image to the target. After training the spatially-conditioned model, we can generate content-consistent human images by iteratively denoising the noisy target image with spatial conditioning derived from the reference image. As demonstrated in Fig. 3, this approach effectively produces human images in novel poses while preserving a high degree of consistency in appearance.

Spatial Conditioning with Causal Feature Interaction. The spatial conditioning strategy ensures the reference and target features lie within the same feature space, facilitating the transfer of reference appearance details to the target through feature interactions within the denoising U-Net. However, this mutual interaction can potentially compromise the integrity of the reference appearance details. To mitigate this risk, we analyze and implement causal feature interaction within the denoising U-Net to enhance consistency in generation. This approach allows reference features to interact solely with themselves, thereby protecting them from the influence of noisy target features while enabling target images to query appearance information from the reference features. We discuss the internal feature interactions within the spatially-conditioned denoising U-Net.

How does the spatially-conditioned reference image influence the content of the generated image? The denoising U-Net of Stable Diffusion comprises multiple basic blocks, each consisting of a residual block [He et al. \(2016\)](#), a self-attention layer, and a cross-attention layer [Vaswani et al. \(2017\)](#). Features from the previous block first pass through the residual block, generating intermediate features. At this stage, feature interactions occur *locally*, particularly in spatially adjacent regions, due to the limited receptive field of the convolution layers. The subsequent self-attention layer facilitates global interactions between the reference and generated image features, allowing the generated image to query comprehensive content information from the reference image through global spatial self-attention. The cross-attention layer, however, only aggregates textual information from the provided textual description to the image features, and thus does not contribute to the interaction between the two types of features. Consequently, with the spatial conditioning strategy, the target image acquires appearance characteristics from the reference image solely through the convolutional and self-attention layers.

How do these two kinds of modules contribute to content consistency? To explore this, we conducted an experiment that eliminated interactions with the convolutional and attention layers in our trained spatial-conditioned model, with results illustrated in Fig. 3(b). Using only the convolutional layers for feature interaction can generate a messy image. Using only the convolutional layers for feature interaction resulted in a chaotic image. In contrast, employing solely the self-attention layer yielded generated images that retained a high degree of similarity to the reference image. This disparity can be attributed to the operational differences between the two types of layers: convolutional layers struggle to transfer reference content to the target image in a very localized manner, while self-attention layers can implicitly warp reference features to target features globally.

Based on this analysis, we conclude that self-attention layers play a dominant role in transferring appearance information from the reference to the target images within the spatial conditioning frame-

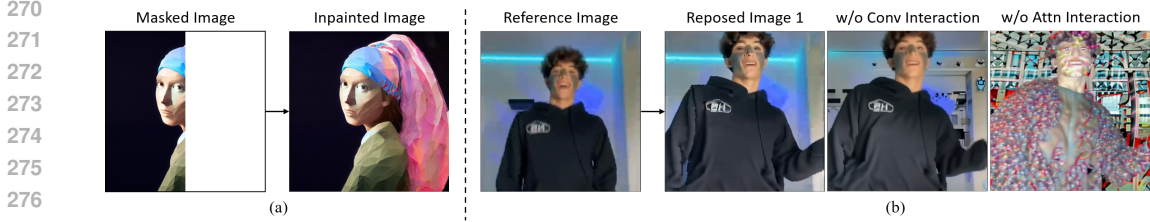


Figure 3: Examples of content consistency through spatial conditioning. (a) Example of zero-shot inpainting with a pretrained Stable Diffusion model Rombach et al. (2022). (b) Results of the spatially-conditioned diffusion model with different configurations. The simple spatial conditioning strategy can generate consistent visual humans, and the attention layers play a key role in achieving such consistency.

work. Therefore, we achieve causal feature interaction by constraining interactions between reference and target features specifically within self-attention layers. More precisely, we implement causal attention within the self-attention layers to enhance the preservation of appearance details from the reference image.

Reference Pose Information Injection. Previous methods Zhang et al. (2023); Mou et al. (2024); Zhao et al. (2024) have shown that an additional trainable network can effectively encode pose conditions into a pretrained diffusion model, resulting in high-quality images that adhere to specified poses. Building on these approaches, we use a small, trainable pose encoder to extract pose features and integrate them into the target image features, thus controlling the poses of the generated human images and videos. Furthermore, we inject the reference pose features into the denoising network along with the spatial conditioning strategy. This further ensures that reference and target features reside within the same feature space, enhancing the correspondence between the two sets of features within each self-attention layer. Consequently, this leads to improved accuracy in pose control.

Practical Implementation. To implement a model with the causal spatial conditioning strategy, we effectively divide the spatially-conditioned generation into two distinct processes as shown in the Fig. 4: reference feature extraction and target image generation. Initially, the reference image x^r is processed through the denoising network to extract the reference features $\epsilon_\theta(x_t^r, t)$. Subsequently, the target image is generated by conditioning on these extracted reference features. Consequently, the objective can be reformulated from Eq. 4 as follows:

$$\mathcal{L}_{\text{scd}} = \mathbb{E}_{x_0, x_0^r, \epsilon, t} (\| \epsilon - \epsilon_\theta(x_t, t, \epsilon_\theta(x_t^r, t, \emptyset)) \|). \quad (1)$$

Note that the t for the reference feature extraction is set to 0 by default. The reference features are injected into the target one with the self-attention layers. Specifically, in i -th self-attention layer of the U-Net, the *query* Q is transformed from the target image features, while the *key* K and *value* V features are the concatenations of the reference and target features: $K = [K^r, K], V = [V^r, V]$. Therefore, the target image can effectively query the appearance features by employing the global attention mechanism described in Eq. 5.

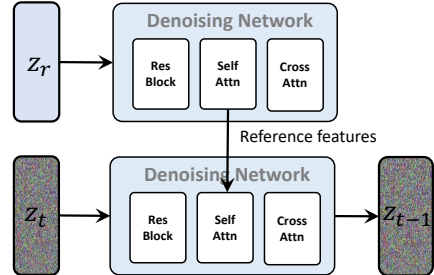


Figure 4: Separating the causal spatial conditioning process into the reference feature extraction and target image generation.

4 EXPERIMENTS

4.1 EXPERIMENTAL SETUP

Datasets. In this study, we employ a combination of publicly available and self-collected datasets for training our model. Specifically, for the public datasets, we use the TikTok Jafarian & Park (2021) and UBCFashion Zablotskaia et al. (2019) datasets to train our video model. The TikTok dataset comprises 350 single-person dance videos, each with a duration ranging from 10 to 15 seconds in length. These videos are sourced from TikTok and primarily showcase a human’s face and

upper body. The UBCFashion dataset contains 600 fashion videos, of which 500 are for training and 100 for testing. Additionally, we have gathered approximately 3,500 dance videos (about 200 humans) from various online sources to further enhance the generalization capability of our proposed framework. As for the evaluation dataset, to be consistent with previous methods Wang et al. (2023); Xu et al. (2023); Chang et al. (2023); Hu et al. (2023), we utilize 10 TikTok-style videos as the test set for evaluating quantitative metrics.

Implementation details. We utilize Stable Diffusion V1.5 Rombach et al. (2022) as our base model for controllable human image generation task, and AnimateDiff Guo et al. (2023) as the video base model for the human animation task. Both models are fine-tuned using the proposed spatial-conditioned diffusion strategy. For training our image model (SCD-I) and video model (SCD-V), we randomly select a single frame from the video to serve as the reference human image. Subsequently, we sample one frame for the SCD-I and 24 frames for the SCD-V as targets. The reference image undergoes a random resized crop, and all frames are adjusted to a resolution of 512×512 . The models are trained using the AdamW optimizer Kingma & Ba (2014) with a learning rate of 1×10^{-5} for 30,000 iterations. The training is conducted on 8 NVIDIA A100 GPUs, employing a batch size of 32 for the SCD-I and 8 for the SCD-V. During the sampling process, we utilize the DDIM sampler Song et al. (2020a) for 25 sampling steps to generate the final outputs. Note that SCD[†] is the original straightforward spatial conditioning model, and SCD is spatial conditioning with causal feature interaction.

Evaluation metrics. In alignment with previous methods Wang et al. (2023); Choi et al. (2021), we employ several image metrics to evaluate the quality of single images, including FID Heusel et al. (2017), SSIM Wang et al. (2004), PSNR Hore & Ziou (2010), and LPIPS Zhang et al. (2018). Additionally, to evaluate the quality of the animated human video, we report video-level metrics such as FID-VID Balaji et al. (2019) and FVD Unterthiner et al. (2018). In addition to these quantitative evaluations, we also present the generated human images and videos for a qualitative comparison.

4.2 COMPARISON TO STATE-OF-THE-ART

We compare the proposed method to the state-of-the-art human animation methods, including (1) GAN-based methods FOMM Siarohin et al. (2019), MRAA Siarohin et al. (2021), and TPS Zhao & Zhang (2022); and (2) recently diffusion-based methods DreamPose Karras et al. (2023), DisCo Wang et al. (2023), AnimateAnyone Hu et al. (2023)¹, MagicPose Chang et al. (2023), and MagicAnimate Xu et al. (2023). We use their official source codes to obtain the animation results, and utilize the evaluation script from DisCo Wang et al. (2023) for fair comparisons.

Quantitative results. Table 1 presents the quantitative performance of various methods on the Tiktok test datasets. Notably, our proposed method, particularly the video-based model SCD-V, achieves highly competitive results. It surpasses state-of-the-art methods such as AnimateAnyone Hu et al. (2023), MagicAnimate Xu et al. (2023), MagicPose Chang et al. (2023), and DisCo Wang et al. (2023) in terms of reconstruction metrics (SSIM, PSNR) and fidelity metrics (LPIPS, FID-VID, FVD). Additionally, our image model SCD-I, also outperforms most existing methods across both image and video metrics. This highly competitive performance can be attributed to the spatially conditioned strategy, which effectively preserves the appearance details of the reference human image. Compared to the Reference-Net-based methods (*i.e.*, MagicAnimate, AnimateAnyone), our methods still demonstrate improvements in most evaluation metrics. These quantitative results underscore the effectiveness and competitiveness of our proposed method in maintaining appearance and identity.

Qualitative results. Figure 5 illustrates the qualitative results of various methods on the Tiktok test set. It is worth noting that the large motions in the dance videos and their length pose a significant challenge in preserving the appearance and identity of the reference human image. Existing methods often produce fragmented results or generate frames that do not align with the given pose, especially when the target pose significantly deviates from the reference human’s pose. In contrast, our method successfully generates unseen parts (*e.g.*, the hands in the first row of Fig. 5) and highly-detailed frames even under challenging poses (as shown in the third row of Fig. 5). Importantly, our approach achieves this while better preserving the appearance and identity of the reference hu-

¹we use the open-sourced implementation to obtain visual results: <https://github.com/MooreThreads/Moore-AnimateAnyone>

Table 1: Quantitative comparison of the proposed method against the recent state-of-the-art methods DisCo Wang et al. (2023), MagicPose Chang et al. (2023), MagicAnimate Xu et al. (2023) and AnimateAnyone Hu et al. (2023). Methods with * directly use the target image as the guidance for the animation, including more information than the densepose and pose skeleton. When calculating the metrics, we resize the input image/video to a resolution 256×256 , following DisCo Wang et al. (2023). Metrics with \uparrow indicate that higher values are better, and vice versa.

Method	Image Mtrics					Video Mtrics	
	FID \downarrow	SSIM \uparrow	PSNR \uparrow	LPIPS \downarrow	L1 \downarrow	FID-VID \downarrow	FVD \downarrow
FOMM* Siarohin et al. (2019)	85.03	0.648	17.26	0.335	3.61E-04	90.09	405.22
MRAA* Siarohin et al. (2021)	54.47	0.672	18.14	0.296	3.21E-04	66.36	284.82
TPS* Zhao & Zhang (2022)	53.78	0.673	18.32	0.299	3.23E-04	72.55	306.17
DreamPose Karras et al. (2023)	72.62	0.511	12.82	0.442	6.88E-04	78.77	551.02
DisCo Wang et al. (2023)	28.31	0.674	16.68	0.285	3.69E-04	55.17	267.75
MagicPose Chang et al. (2023)	26.67	0.692	17.03	0.270	3.33E-04	61.73	230.88
MagicAnimate Xu et al. (2023)	32.09	0.714	18.22	0.239	3.13E-04	21.75	179.07
AnimateAnyone Hu et al. (2023)	-	0.718	-	0.285	-	-	171.9
SCD-I (Ours)	33.63	0.726	18.64	0.240	2.72E-04	33.15	153.99
SCD-V (Ours)	34.44	0.731	18.81	0.236	2.75E-04	15.58	136.60

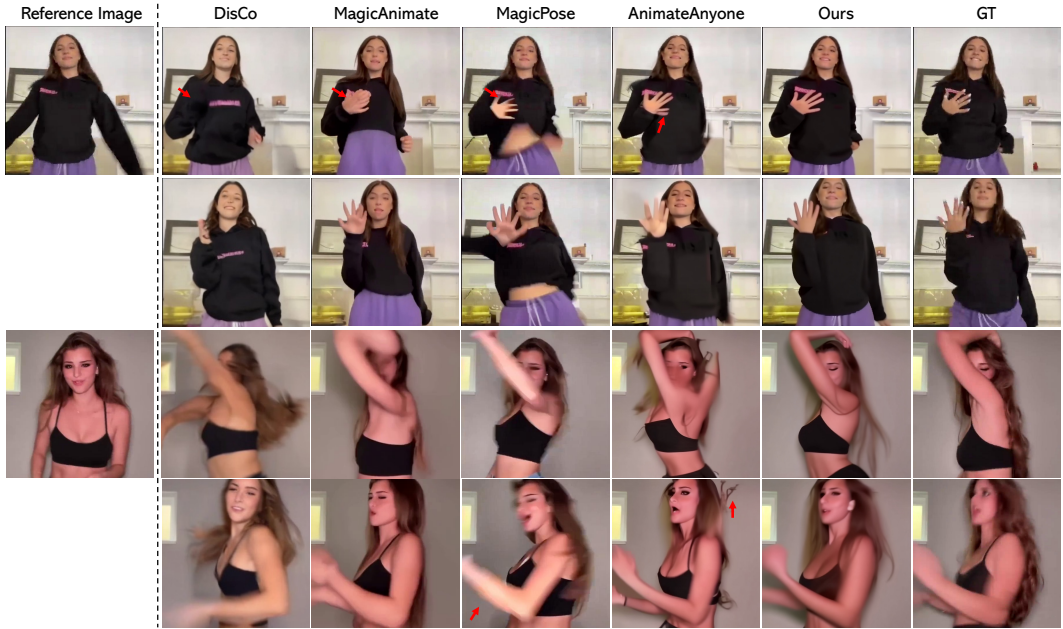


Figure 5: Qualitative comparison results against state-of-the-art human animation methods on the TikTok datasets Wang et al. (2023). The proposed method can generate high-quality human videos complying with the given pose sequence.

man. These highly competitive results further demonstrate the effectiveness of the proposed method, which harnesses the denoising network’s capacity to encode appearance information independently, ensuring the reference and target features reside in the same feature space.

4.3 ABLATION STUDY

To further validate the effectiveness of our model’s design, we conduct ablation studies on our proposed method, focusing on the conditioning strategy and the training data.

Spatial conditioning strategy. To evaluate the effectiveness of the proposed spatial conditioning strategy for consistent human image and video generation, we incorporate reference image informa-

Table 2: Ablation results of the proposed method. The best results in each part are bold, and the default setting is grayed. SCD[†] means the straightforward spatial conditioning strategy without causal feature interaction.

	FID ↓	SSIM ↑	PSNR ↑	LPIPS ↓	L1 ↓	FID-VID ↓	FVD ↓
CLIP embedding	79.51	0.474	12.88	0.484	6.84E-04	106.26	690.50
Channel concatenation	64.60	0.577	15.09	0.390	5.15E-04	80.92	590.36
Reference-Net (w/o SD init)	48.99	0.690	16.87	0.280	3.65E-04	40.60	303.63
Reference-Net	41.55	0.720	18.18	0.247	3.02E-04	32.44	172.48
SCD-I [†] (w/o ref pose)	34.82	0.721	18.14	0.249	3.13E-04	36.49	218.93
SCD-I [†]	33.13	0.728	18.59	0.242	2.77E-04	32.43	164.83
SCD-I (w/o ref pose)	35.84	0.728	18.58	0.242	2.70E-04	32.79	162.75
SCD-I	33.63	0.726	18.64	0.240	2.72E-04	33.15	153.99



Figure 6: Ablation of different reference image conditioning methods and the key components of the proposed method.

tion using the following alternatives: **1)** CLIP [Radford et al. \(2021\)](#) embedding conditioning, which employs a pretrained CLIP image encoder to extract appearance features and inject them into the denoising U-Net via cross-attention; **2)** Channel concatenation conditioning, which concatenates the reference image latents with the noise map along the channel axis and directly inputs them into the denoising network; **3)** Reference-Net, which utilizes an additional trainable version of the denoising network to extract appearance features, incorporating a reference attention mechanism for injection.

The results are presented in Tab. 2 and Fig. 6. Notably, the CLIP conditioning strategy yields the lowest performance metrics. We hypothesize that, since CLIP is trained on image-text pairs to align the two modalities, it excels at capturing high-level semantic features but struggles to retain the fine-grained appearance details of the reference image. Although both DreamPose [Karras et al. \(2023\)](#) and Disco [Wang et al. \(2023\)](#) employ similar approaches to preserve appearance and identity information, additional strategies are necessary to maintain finer details. For instance, Disco employs a disentangled control strategy and is pretrained on a substantial amount of data to ensure background consistency, while DreamPose conducts model fine-tuning for each reference image to achieve consistent generation. Nevertheless, both methods still fail to preserve the fine-grained details of the reference image (as shown in Fig. 5). The channel concatenation strategy outperforms the CLIP conditioning by better preserving the background but struggles to generate humans in new poses, particularly with limited training data. In contrast, the Reference-Net (as used in AnimateAnyone [Hu et al. \(2023\)](#) and MagicAnimate [Xu et al. \(2023\)](#)) achieves significantly higher metrics and improved visual quality compared to the aforementioned strategies, owing to the fine-grained features extracted by the reference network. However, this approach requires training an additional reference feature extractor and aligning the reference features to the target features. Conversely, our proposed spatial conditioning strategy achieves slightly better performance than the Reference-Net by leveraging the denoising network’s inherent capabilities for extracting reference appearance information and generating target images.

Causal Feature Interaction. By augmenting the original spatial conditioning with causal feature interaction to more effectively preserve reference appearance information, we observe additional improvements in reconstruction quality metrics, surpassing those of existing conditioning methods (CLIP, channel concatenation, and Reference-Net). These results demonstrate that this strategy successfully mitigates perturbations from noisy target features, thereby enhancing the preservation of appearance information from the reference image and yielding higher reconstruction metrics.

Although our practical implementation of the causal feature interaction is similar to the Reference-Net, our spatial conditioning strategy ensures the reference appearance features reside in the same

486 feature space as the features of generating the target image using the unified denoising network.
487 The unified feature space is important for content consistency. A straightforward example is that
488 when randomly initializing the Reference-Net rather than using original Stable Diffusion weights,
489 the model performance drastically drops, especially the reconstruction metrics, as shown in Tab. 2,
490 since there is a huge burden in aligning the features from the Reference-Net and the denoising
491 network during the training process.

492 While our practical implementation of causal feature interaction is similar to that of the Reference-
493 Net, our spatial conditioning strategy ensures that the reference appearance features reside in the
494 same feature space within the denoising network. This unified feature space is critical for maintain-
495 ing content consistency. A clear illustration of this is shown in Tab. 2. When we randomly initialize
496 the Reference-Net instead of using the original Stable Diffusion weights, the model’s performance
497 significantly deteriorates, particularly regarding reconstruction metrics. This decline occurs due to
498 the substantial burden of aligning the features from the Reference-Net with those of the denoising
499 network during the training process.

500 **Reference pose injection.** We also incorporate reference pose information to enhance the align-
501 ment between reference and target features, enhancing their correspondence for more precise pose
502 control. As shown in Tab. 2, the absence of reference pose information injection results in a decline
503 in reconstruction metrics, such as PSNR and SSIM. Furthermore, as illustrated in Fig. 6, without
504 reference pose, the model may produce incorrect target human images. In contrast, injecting refer-
505 ence pose information along with the reference image into the denoising network further ensures
506 the reference and target features reside in the same feature space. Consequently, this strategy further
507 facilitates the generation of target images that better comply with the desired pose.

509 4.4 DISCUSSION AND LIMITATIONS

511 **More Applications.** Our proposed spatial conditioning strategy can also be effectively applied to
512 other tasks that require appearance preservation, such as visual try-on and face reenactment. For
513 instance, when training our image model SCD-I with the visual try-on dataset VITON-HD [Choi](#)
514 [et al. \(2021\)](#), our method facilitates high-quality visual try-on, as illustrated in Fig. 1. The fine-
515 grained textures and text from the garment image can be perfectly transferred to the model, further
516 demonstrating the effectiveness of the proposed self-conditioned strategy. Additional results can be
517 found in the Appendix.

518 **Limitations.** Despite its effectiveness, our method has certain limitations, particularly in scenarios
519 where the background is complex and the target pose significantly deviates from the reference human
520 image. For instance, during extreme zooming in or out, the appearance and identity may not be
521 perfectly preserved. Additionally, our method struggles to generate perfect faces and hands. We
522 believe that these challenges can be addressed by collecting more high-quality data and employing
523 advanced training strategies. Furthermore, we can apply the spatial conditioning strategy to the more
524 powerful base image and video diffusion models, such as Stable Video Diffusion [Blattmann et al.](#)
525 [\(2023a\)](#) and Stable Diffusion 3 [Esser et al. \(2024\)](#), to achieve improved performance.

527 5 CONCLUSION

528
529
530 In this paper, we explore the generation of consistent human-centric visual content through a self-
531 conditioning strategy. We frame consistent reference-based controllable human image and video
532 generation as a spatial inpainting task, in which the desired content is spatially inpainted under
533 the conditioning of a reference human image. Additionally, we propose a causal spatial condition-
534 ing strategy that constrains the interaction between reference and target features causally, thereby
535 further preserving the appearance information of the given reference images for enhanced consis-
536 tency. By leveraging the inherent capabilities of the denoising network for appearance detail extrac-
537 tion and conditioned generation, our approach is both straightforward and effective in maintaining
538 fine-grained appearance details and the identity of the reference human image. Experimental re-
539 sults validate the effectiveness and competitiveness of our method compared to existing approaches.
We believe that this self-conditioning strategy holds the potential to establish a new paradigm for
reference-based generation.

REFERENCES

- 540
541
542 Yogesh Balaji, Martin Renqiang Min, Bing Bai, Rama Chellappa, and Hans Peter Graf. Conditional
543 gan with discriminative filter generation for text-to-video synthesis. In *IJCAI*, volume 1, pp. 2,
544 2019. 7
- 545 Ankan Kumar Bhunia, Salman Khan, Hisham Cholakkal, Rao Muhammad Anwer, Jorma Laakso-
546 nen, Mubarak Shah, and Fahad Shahbaz Khan. Person image synthesis via denoising diffusion
547 model. In *Proceedings of the IEEE/CVF Conference on Computer Vision and Pattern Recogni-
548 tion*, pp. 5968–5976, 2023. 1, 4
- 549
550 Andreas Blattmann, Tim Dockhorn, Sumith Kulal, Daniel Mendelevitch, Maciej Kilian, Dominik
551 Lorenz, Yam Levi, Zion English, Vikram Voleti, Adam Letts, et al. Stable video diffusion: Scaling
552 latent video diffusion models to large datasets. *arXiv preprint arXiv:2311.15127*, 2023a. 1, 3, 10
- 553 Andreas Blattmann, Robin Rombach, Huan Ling, Tim Dockhorn, Seung Wook Kim, Sanja Fidler,
554 and Karsten Kreis. Align your latents: High-resolution video synthesis with latent diffusion mod-
555 els. In *Proceedings of the IEEE/CVF Conference on Computer Vision and Pattern Recognition*,
556 pp. 22563–22575, 2023b. 3
- 557
558 Mingdeng Cao, Xintao Wang, Zhongang Qi, Ying Shan, Xiaohu Qie, and Yinqiang Zheng. Mas-
559 actrl: Tuning-free mutual self-attention control for consistent image synthesis and editing. In
560 *Proceedings of the IEEE/CVF International Conference on Computer Vision*, pp. 22560–22570,
561 2023. 2, 3, 16
- 562 Mathilde Caron, Hugo Touvron, Ishan Misra, Hervé Jégou, Julien Mairal, Piotr Bojanowski, and
563 Armand Joulin. Emerging properties in self-supervised vision transformers. In *Proceedings of
564 the International Conference on Computer Vision (ICCV)*, 2021. 4
- 565
566 Duygu Ceylan, Chun-Hao P Huang, and Niloy J Mitra. Pix2video: Video editing using image
567 diffusion. In *Proceedings of the IEEE/CVF International Conference on Computer Vision*, pp.
568 23206–23217, 2023. 3
- 569
570 Caroline Chan, Shiry Ginosar, Tinghui Zhou, and Alexei A Efros. Everybody dance now. In *Pro-
571 ceedings of the IEEE/CVF international conference on computer vision*, pp. 5933–5942, 2019.
572 1
- 573 Di Chang, Yichun Shi, Quankai Gao, Jessica Fu, Hongyi Xu, Guoxian Song, Qing Yan, Xiao Yang,
574 and Mohammad Soleymani. Magicedance: Realistic human dance video generation with motions
575 & facial expressions transfer. *arXiv preprint arXiv:2311.12052*, 2023. 1, 3, 7, 8
- 576
577 Xi Chen, Lianghua Huang, Yu Liu, Yujun Shen, Deli Zhao, and Hengshuang Zhao. Anydoor: Zero-
578 shot object-level image customization. *arXiv preprint arXiv:2307.09481*, 2023. 2, 4
- 579
580 Seunghwan Choi, Sunghyun Park, Minsoo Lee, and Jaegul Choo. Viton-hd: High-resolution virtual
581 try-on via misalignment-aware normalization. In *Proceedings of the IEEE/CVF conference on
582 computer vision and pattern recognition*, pp. 14131–14140, 2021. 1, 7, 10, 16
- 583
584 Yisol Choi, Sangkyung Kwak, Kyungmin Lee, Hyungwon Choi, and Jinwoo Shin. Improving dif-
585 fusion models for virtual try-on. *arXiv preprint arXiv:2403.05139*, 2024. 4, 17
- 586
587 Prafulla Dhariwal and Alexander Nichol. Diffusion models beat gans on image synthesis. *Advances
588 in neural information processing systems*, 34:8780–8794, 2021. 1
- 589
590 Patrick Esser, Sumith Kulal, Andreas Blattmann, Rahim Entezari, Jonas Müller, Harry Saini, Yam
591 Levi, Dominik Lorenz, Axel Sauer, Frederic Boesel, et al. Scaling rectified flow transformers for
592 high-resolution image synthesis. In *Forty-first International Conference on Machine Learning*,
593 2024. 10
- 594
595 Rinon Gal, Yuval Alaluf, Yuval Atzmon, Or Patashnik, Amit H Bermano, Gal Chechik, and Daniel
596 Cohen-Or. An image is worth one word: Personalizing text-to-image generation using textual
597 inversion. *arXiv preprint arXiv:2208.01618*, 2022. 3

- 594 Yuying Ge, Yibing Song, Ruimao Zhang, Chongjian Ge, Wei Liu, and Ping Luo. Parser-free virtual
595 try-on via distilling appearance flows. In *Proceedings of the IEEE/CVF conference on computer
596 vision and pattern recognition*, pp. 8485–8493, 2021. 1
- 597 Michal Geyer, Omer Bar-Tal, Shai Bagon, and Tali Dekel. Tokenflow: Consistent diffusion features
598 for consistent video editing. *arXiv preprint arXiv:2307.10373*, 2023. 3
- 600 Junhong Gou, Siyu Sun, Jianfu Zhang, Jianlou Si, Chen Qian, and Liqing Zhang. Taming the power
601 of diffusion models for high-quality virtual try-on with appearance flow. In *Proceedings of the
602 31st ACM International Conference on Multimedia*, pp. 7599–7607, 2023. 4
- 603 Yuwei Guo, Ceyuan Yang, Anyi Rao, Yaohui Wang, Yu Qiao, Dahua Lin, and Bo Dai. Animatediff:
604 Animate your personalized text-to-image diffusion models without specific tuning. *arXiv preprint
605 arXiv:2307.04725*, 2023. 1, 3, 7
- 607 Xintong Han, Zuxuan Wu, Zhe Wu, Ruichi Yu, and Larry S Davis. Viton: An image-based virtual
608 try-on network. In *Proceedings of the IEEE conference on computer vision and pattern recogni-
609 tion*, pp. 7543–7552, 2018. 1
- 610 Kaiming He, Xiangyu Zhang, Shaoqing Ren, and Jian Sun. Deep residual learning for image recog-
611 nition. In *Proceedings of the IEEE conference on computer vision and pattern recognition*, pp.
612 770–778, 2016. 5
- 613 Amir Hertz, Ron Mokady, Jay Tenenbaum, Kfir Aberman, Yael Pritch, and Daniel Cohen-Or.
614 Prompt-to-prompt image editing with cross attention control. *arXiv preprint arXiv:2208.01626*,
615 2022. 3
- 617 Martin Heusel, Hubert Ramsauer, Thomas Unterthiner, Bernhard Nessler, and Sepp Hochreiter.
618 Gans trained by a two time-scale update rule converge to a local nash equilibrium. *Advances in
619 neural information processing systems*, 30, 2017. 7
- 620 Jonathan Ho, Ajay Jain, and Pieter Abbeel. Denoising diffusion probabilistic models. *Advances in
621 neural information processing systems*, 33:6840–6851, 2020. 1, 3, 16
- 623 Jonathan Ho, William Chan, Chitwan Saharia, Jay Whang, Ruiqi Gao, Alexey Gritsenko, Diederik P
624 Kingma, Ben Poole, Mohammad Norouzi, David J Fleet, et al. Imagen video: High definition
625 video generation with diffusion models. *arXiv preprint arXiv:2210.02303*, 2022a. 3
- 626 Jonathan Ho, Tim Salimans, Alexey Gritsenko, William Chan, Mohammad Norouzi, and David J
627 Fleet. Video diffusion models. *Advances in Neural Information Processing Systems*, 35:8633–
628 8646, 2022b. 3
- 629 Wenyi Hong, Ming Ding, Wendi Zheng, Xinghan Liu, and Jie Tang. Cogvideo: Large-scale pre-
630 training for text-to-video generation via transformers. *arXiv preprint arXiv:2205.15868*, 2022.
631 3
- 633 Alain Hore and Djemel Ziou. Image quality metrics: Psnr vs. ssim. In *2010 20th international
634 conference on pattern recognition*, pp. 2366–2369. IEEE, 2010. 7
- 635 Li Hu, Xin Gao, Peng Zhang, Ke Sun, Bang Zhang, and Liefeng Bo. Animate anyone:
636 Consistent and controllable image-to-video synthesis for character animation. *arXiv preprint
637 arXiv:2311.17117*, 2023. 1, 2, 3, 4, 7, 8, 9
- 638 Lianghua Huang, Di Chen, Yu Liu, Yujun Shen, Deli Zhao, and Jingren Zhou. Composer: Creative
639 and controllable image synthesis with composable conditions. *arXiv preprint arXiv:2302.09778*,
640 2023. 4
- 642 Yasamin Jafarian and Hyun Soo Park. Learning high fidelity depths of dressed humans by watching
643 social media dance videos. In *Proceedings of the IEEE/CVF Conference on Computer Vision and
644 Pattern Recognition*, pp. 12753–12762, 2021. 6
- 645 Johanna Karras, Aleksander Holynski, Ting-Chun Wang, and Ira Kemelmacher-Shlizerman. Dream-
646 pose: Fashion video synthesis with stable diffusion. In *Proceedings of the IEEE/CVF Interna-
647 tional Conference on Computer Vision*, pp. 22680–22690, 2023. 1, 2, 4, 7, 8, 9

- 648 Levon Khachatryan, Andranik Movsisyan, Vahram Tadevosyan, Roberto Henschel, Zhangyang
649 Wang, Shant Navasardyan, and Humphrey Shi. Text2video-zero: Text-to-image diffusion models
650 are zero-shot video generators. In *Proceedings of the IEEE/CVF International Conference on*
651 *Computer Vision*, pp. 15954–15964, 2023. [2](#), [3](#), [16](#)
- 652 Jeongho Kim, Gyojung Gu, Minhoo Park, Sunghyun Park, and Jaegul Choo. Stableviton: Learning
653 semantic correspondence with latent diffusion model for virtual try-on, 2023. [4](#), [17](#)
- 654 Diederik P Kingma and Jimmy Ba. Adam: A method for stochastic optimization. *arXiv preprint*
655 *arXiv:1412.6980*, 2014. [7](#), [16](#)
- 656 Shaoteng Liu, Yuechen Zhang, Wenbo Li, Zhe Lin, and Jiaya Jia. Video-p2p: Video editing with
657 cross-attention control. *arXiv preprint arXiv:2303.04761*, 2023. [3](#)
- 658 Chenlin Meng, Yutong He, Yang Song, Jiaming Song, Jiajun Wu, Jun-Yan Zhu, and Stefano Ermon.
659 Sdedit: Guided image synthesis and editing with stochastic differential equations. *arXiv preprint*
660 *arXiv:2108.01073*, 2021. [3](#)
- 661 Chong Mou, Xintao Wang, Liangbin Xie, Yanze Wu, Jian Zhang, Zhongang Qi, and Ying Shan.
662 T2i-adapter: Learning adapters to dig out more controllable ability for text-to-image diffusion
663 models. In *Proceedings of the AAAI Conference on Artificial Intelligence*, volume 38, pp. 4296–
664 4304, 2024. [3](#), [6](#)
- 665 Alex Nichol, Prafulla Dhariwal, Aditya Ramesh, Pranav Shyam, Pamela Mishkin, Bob McGrew,
666 Ilya Sutskever, and Mark Chen. Glide: Towards photorealistic image generation and editing with
667 text-guided diffusion models. *arXiv preprint arXiv:2112.10741*, 2021. [3](#), [16](#)
- 668 Alexander Quinn Nichol and Prafulla Dhariwal. Improved denoising diffusion probabilistic models.
669 In *International conference on machine learning*, pp. 8162–8171. PMLR, 2021. [16](#)
- 670 William Peebles and Saining Xie. Scalable diffusion models with transformers. In *Proceedings of*
671 *the IEEE/CVF International Conference on Computer Vision*, pp. 4195–4205, 2023. [1](#), [3](#)
- 672 Chenyang Qi, Xiaodong Cun, Yong Zhang, Chenyang Lei, Xintao Wang, Ying Shan, and Qifeng
673 Chen. Fatezero: Fusing attentions for zero-shot text-based video editing. In *Proceedings of the*
674 *IEEE/CVF International Conference on Computer Vision*, pp. 15932–15942, 2023. [3](#)
- 675 Alec Radford, Jong Wook Kim, Chris Hallacy, Aditya Ramesh, Gabriel Goh, Sandhini Agarwal,
676 Girish Sastry, Amanda Askell, Pamela Mishkin, Jack Clark, et al. Learning transferable visual
677 models from natural language supervision. In *International conference on machine learning*, pp.
678 8748–8763. PMLR, 2021. [2](#), [4](#), [9](#)
- 679 Aditya Ramesh, Prafulla Dhariwal, Alex Nichol, Casey Chu, and Mark Chen. Hierarchical text-
680 conditional image generation with clip latents. *arXiv preprint arXiv:2204.06125*, 1(2):3, 2022.
681 [3](#)
- 682 Yurui Ren, Ge Li, Shan Liu, and Thomas H Li. Deep spatial transformation for pose-guided person
683 image generation and animation. *IEEE Transactions on Image Processing*, 29:8622–8635, 2020.
684 [1](#)
- 685 Yurui Ren, Xiaoqing Fan, Ge Li, Shan Liu, and Thomas H Li. Neural texture extraction and distri-
686 bution for controllable person image synthesis. In *Proceedings of the IEEE/CVF conference on*
687 *computer vision and pattern recognition*, pp. 13535–13544, 2022. [1](#)
- 688 Robin Rombach, Andreas Blattmann, Dominik Lorenz, Patrick Esser, and Björn Ommer. High-
689 resolution image synthesis with latent diffusion models. In *Proceedings of the IEEE/CVF con-*
690 *ference on computer vision and pattern recognition*, pp. 10684–10695, 2022. [1](#), [3](#), [5](#), [6](#), [7](#), [16](#),
691 [17](#)
- 692 Olaf Ronneberger, Philipp Fischer, and Thomas Brox. U-net: Convolutional networks for biomed-
693 ical image segmentation. In *Medical image computing and computer-assisted intervention–*
694 *MICCAI 2015: 18th international conference, Munich, Germany, October 5-9, 2015, proceed-*
695 *ings, part III 18*, pp. 234–241. Springer, 2015. [16](#)

- 702 Nataniel Ruiz, Yuanzhen Li, Varun Jampani, Yael Pritch, Michael Rubinstein, and Kfir Aberman.
703 Dreambooth: Fine tuning text-to-image diffusion models for subject-driven generation. In *Pro-*
704 *ceedings of the IEEE/CVF Conference on Computer Vision and Pattern Recognition*, pp. 22500–
705 22510, 2023. 3
- 706
707 Chitwan Saharia, William Chan, Saurabh Saxena, Lala Li, Jay Whang, Emily L Denton, Kamyar
708 Ghasemipour, Raphael Gontijo Lopes, Burcu Karagol Ayan, Tim Salimans, et al. Photorealistic
709 text-to-image diffusion models with deep language understanding. *Advances in neural informa-*
710 *tion processing systems*, 35:36479–36494, 2022. 1, 3
- 711
712 Aliaksandr Siarohin, Stéphane Lathuilière, Sergey Tulyakov, Elisa Ricci, and Nicu Sebe. First order
713 motion model for image animation. *Advances in neural information processing systems*, 32, 2019.
714 1, 7, 8
- 715
716 Aliaksandr Siarohin, Oliver J Woodford, Jian Ren, Menglei Chai, and Sergey Tulyakov. Motion rep-
717 resentations for articulated animation. In *Proceedings of the IEEE/CVF Conference on Computer*
718 *Vision and Pattern Recognition*, pp. 13653–13662, 2021. 7, 8
- 719
720 Uriel Singer, Adam Polyak, Thomas Hayes, Xi Yin, Jie An, Songyang Zhang, Qiyuan Hu, Harry
721 Yang, Oron Ashual, Oran Gafni, et al. Make-a-video: Text-to-video generation without text-video
722 data. *arXiv preprint arXiv:2209.14792*, 2022. 3
- 723
724 Jascha Sohl-Dickstein, Eric Weiss, Niru Maheswaranathan, and Surya Ganguli. Deep unsupervised
725 learning using nonequilibrium thermodynamics. In *International conference on machine learn-*
726 *ing*, pp. 2256–2265. PMLR, 2015. 3, 16
- 727
728 Jiaming Song, Chenlin Meng, and Stefano Ermon. Denoising diffusion implicit models. *arXiv*
729 *preprint arXiv:2010.02502*, 2020a. 7, 16
- 730
731 Yang Song and Stefano Ermon. Generative modeling by estimating gradients of the data distribution.
732 *Advances in neural information processing systems*, 32, 2019. 3, 16
- 733
734 Yang Song, Jascha Sohl-Dickstein, Diederik P Kingma, Abhishek Kumar, Stefano Ermon, and Ben
735 Poole. Score-based generative modeling through stochastic differential equations. *arXiv preprint*
736 *arXiv:2011.13456*, 2020b. 3, 16
- 737
738 Narek Tumanyan, Michal Geyer, Shai Bagon, and Tali Dekel. Plug-and-play diffusion features for
739 text-driven image-to-image translation. In *Proceedings of the IEEE/CVF Conference on Com-*
740 *puter Vision and Pattern Recognition*, pp. 1921–1930, 2023. 3, 16
- 741
742 Thomas Unterthiner, Sjoerd Van Steenkiste, Karol Kurach, Raphael Marinier, Marcin Michalski,
743 and Sylvain Gelly. Towards accurate generative models of video: A new metric & challenges.
744 *arXiv preprint arXiv:1812.01717*, 2018. 7
- 745
746 Ashish Vaswani, Noam Shazeer, Niki Parmar, Jakob Uszkoreit, Llion Jones, Aidan N Gomez,
747 Łukasz Kaiser, and Illia Polosukhin. Attention is all you need. *Advances in neural informa-*
748 *tion processing systems*, 30, 2017. 5, 16
- 749
750 Tan Wang, Linjie Li, Kevin Lin, Chung-Ching Lin, Zhengyuan Yang, Hanwang Zhang, Zicheng
751 Liu, and Lijuan Wang. Disco: Disentangled control for referring human dance generation in real
752 world. *arXiv e-prints*, pp. arXiv–2307, 2023. 1, 4, 7, 8, 9
- 753
754 Zhou Wang, Alan C Bovik, Hamid R Sheikh, and Eero P Simoncelli. Image quality assessment:
755 from error visibility to structural similarity. *IEEE transactions on image processing*, 13(4):600–
612, 2004. 7
- 756
757 Jay Zhangjie Wu, Yixiao Ge, Xintao Wang, Stan Weixian Lei, Yuchao Gu, Yufei Shi, Wynne Hsu,
758 Ying Shan, Xiaohu Qie, and Mike Zheng Shou. Tune-a-video: One-shot tuning of image diffusion
759 models for text-to-video generation. In *Proceedings of the IEEE/CVF International Conference*
760 *on Computer Vision*, pp. 7623–7633, 2023. 3

- 756 Zhenyu Xie, Zaiyu Huang, Xin Dong, Fuwei Zhao, Haoye Dong, Xijin Zhang, Feida Zhu, and
757 Xiaodan Liang. Gp-vton: Towards general purpose virtual try-on via collaborative local-flow
758 global-parsing learning. In *Proceedings of the IEEE/CVF Conference on Computer Vision and
759 Pattern Recognition*, pp. 23550–23559, 2023. 1
- 760 Yuhao Xu, Tao Gu, Weifeng Chen, and Chengcai Chen. Ootdiffusion: Outfitting fusion based latent
761 diffusion for controllable virtual try-on. *arXiv preprint arXiv:2403.01779*, 2024. 4, 17
- 762 Zhongcong Xu, Jianfeng Zhang, Jun Hao Liew, Hanshu Yan, Jia-Wei Liu, Chenxu Zhang, Jiashi
763 Feng, and Mike Zheng Shou. Magicanimate: Temporally consistent human image animation
764 using diffusion model. *arXiv preprint arXiv:2311.16498*, 2023. 1, 2, 3, 4, 7, 8, 9
- 765 Binxin Yang, Shuyang Gu, Bo Zhang, Ting Zhang, Xuejin Chen, Xiaoyan Sun, Dong Chen, and
766 Fang Wen. Paint by example: Exemplar-based image editing with diffusion models. In *Pro-
767 ceedings of the IEEE/CVF Conference on Computer Vision and Pattern Recognition*, pp. 18381–
768 18391, 2023a. 4
- 769 Han Yang, Ruimao Zhang, Xiaobao Guo, Wei Liu, Wangmeng Zuo, and Ping Luo. Towards photo-
770 realistic virtual try-on by adaptively generating-preserving image content. In *Proceedings of the
771 IEEE/CVF conference on computer vision and pattern recognition*, pp. 7850–7859, 2020. 1
- 772 Shuai Yang, Yifan Zhou, Ziwei Liu, and Chen Change Loy. Rerender a video: Zero-shot text-guided
773 video-to-video translation. In *SIGGRAPH Asia 2023 Conference Papers*, pp. 1–11, 2023b. 3
- 774 Polina Zablotskaia, Aliaksandr Siarohin, Bo Zhao, and Leonid Sigal. Dwnet: Dense warp-based
775 network for pose-guided human video generation. *arXiv preprint arXiv:1910.09139*, 2019. 6
- 776 Lvmin Zhang, Anyi Rao, and Maneesh Agrawala. Adding conditional control to text-to-image
777 diffusion models. In *Proceedings of the IEEE/CVF International Conference on Computer Vision*,
778 pp. 3836–3847, 2023. 2, 3, 6
- 779 Pengze Zhang, Lingxiao Yang, Jian-Huang Lai, and Xiaohua Xie. Exploring dual-task correla-
780 tion for pose guided person image generation. In *Proceedings of the IEEE/CVF Conference on
781 Computer Vision and Pattern Recognition*, pp. 7713–7722, 2022. 1
- 782 Richard Zhang, Phillip Isola, Alexei A Efros, Eli Shechtman, and Oliver Wang. The unreasonable
783 effectiveness of deep features as a perceptual metric. In *Proceedings of the IEEE conference on
784 computer vision and pattern recognition*, pp. 586–595, 2018. 7
- 785 Jian Zhao and Hui Zhang. Thin-plate spline motion model for image animation. In *Proceedings of
786 the IEEE/CVF Conference on Computer Vision and Pattern Recognition*, pp. 3657–3666, 2022.
787 1, 7, 8
- 788 Shihao Zhao, Dongdong Chen, Yen-Chun Chen, Jianmin Bao, Shaozhe Hao, Lu Yuan, and Kwan-
789 Yee K Wong. Uni-controlnet: All-in-one control to text-to-image diffusion models. *Advances in
790 Neural Information Processing Systems*, 36, 2024. 3, 6
- 791 Luyang Zhu, Dawei Yang, Tyler Zhu, Fitsum Reda, William Chan, Chitwan Saharia, Mohammad
792 Norouzi, and Ira Kemelmacher-Shlizerman. Tryondiffusion: A tale of two unets. In *Proceedings
793 of the IEEE/CVF Conference on Computer Vision and Pattern Recognition*, pp. 4606–4615, 2023.
794 4
- 795 Shenhao Zhu, Junming Leo Chen, Zuozhuo Dai, Yinghui Xu, Xun Cao, Yao Yao, Hao Zhu, and Siyu
796 Zhu. Champ: Controllable and consistent human image animation with 3d parametric guidance.
797 *arXiv preprint arXiv:2403.14781*, 2024. 4
- 800
801
802
803
804
805
806
807
808
809

A APPENDIX

A.1 BACKGROUND OF STABLE DIFFUSION

Diffusion models Sohl-Dickstein et al. (2015); Ho et al. (2020); Song et al. (2020a); Nichol & Dhariwal (2021) and score-based generative models Song & Ermon (2019); Song et al. (2020b) are a class of probabilistic generative frameworks that learn to reverse the process that gradually degrades the training data distribution. A diffusion model contains a forward and a backward process that adds the noise and removes the noise of the data samples, respectively. During training, the data sample x_0 is perturbed to a noisy one x_t by a pre-defined degradation schedule $\alpha_{1:T} \in (0, 1]^T$:

$$q(x_t|x_0) = \mathcal{N}(x_t; \sqrt{\alpha_t}x_0, (1 - \alpha_t)\mathbf{I}); \quad (2)$$

so we can obtain x_t from the clean sample x_0 and a Gaussian noise ϵ :

$$x_t = \sqrt{\alpha_t}x_0 + \sqrt{1 - \alpha_t}\epsilon, \quad (3)$$

where $\epsilon \in \mathcal{N}(0, \mathbf{I})$, and x_T coverages to a standard Gaussian for all x_0 . The reverse process tries to remove the added noise from the noisy sample x_t . To achieve this, usually, a denoising network ϵ_θ is trained with the objective:

$$\mathcal{L}_{\text{simple}} = \mathbb{E}_{x_0, \epsilon, t} (\| \epsilon - \epsilon_\theta(x_t, t) \|). \quad (4)$$

Once the denoising network has been trained, x_0 can be obtained by iteratively performing the denoising process by first sampling x_T from a standard Gaussian. The denoising model is typically realized as a UNet Ronneberger et al. (2015), and the Transformer Vaswani et al. (2017) is further employed currently. Meanwhile, conditioned generation can be achieved when integrating additional conditions like textual description into the denoising model.

Attention mechanism is widely integrated into UNet- and Transformer-based diffusion models. Usually, both self-attention and cross-attention are employed in a text-conditioned diffusion model:

$$\text{Attention}(Q, K, V) = \text{Softmax}\left(\frac{QK^T}{\sqrt{d}}\right)V, \quad (5)$$

where Q is the query feature projected from the noisy image feature, and K, V serve as the key and value features projected image features (self-attention) or textual feature (cross-attention). d is the dimension of projected features. With cross-attention layers, textual information can be fused to the generation process, enabling diffusion models to generate images or videos complied with the given textual descriptions Nichol et al. (2021); Rombach et al. (2022). While the self-attention layers try to rearrange the image features, thus they play a crucial role in determining the structure and shape details of the synthesized image Tumanyan et al. (2023). Moreover, in a pre-trained image diffusion, the self-attention layer can be adapted to a crossing one to generate content-consistent images Cao et al. (2023) or temporal-consistent videos Khachatryan et al. (2023).

A.2 SCD FOR VISUAL TRY-ON

Datasets and implementation details. Our method can also applied to the visual try-on task to generate garment-consistent human images. To validate this, we train our image model SCD-I² on the VITON-HD Choi et al. (2021) dataset, which contains 11,647 half-body model images and corresponding garment images at 1024×768 resolutions for training. Note that we only add noise to the garment region in the human image x_0 as input for the denoising network, with the provided garment mark M in the dataset:

$$x_t = (\sqrt{\alpha_t}x_0 + \sqrt{1 - \alpha_t}\epsilon) * M + x_0 + (1 - M). \quad (6)$$

We also apply the garment mask during the loss calculation to ensure the model can inpaint the masked region conditioned on the unmasked human image and the garment image. The model is trained with a learning rate 1×10^{-5} for 30,000 iterations, and Adam Kingma & Ba (2014) is employed to optimize model parameters with a batch size of 8.

²We don't apply the reference pose information injection strategy since the pose of the garment image cannot be extracted.

864 **Comparison to State-of-the-Art.** We compare the proposed model to the state-of-the-art visual
865 try-on methods, including GAN-based method HR-VITON Rombach et al. (2022), and recently
866 proposed diffusion model-based methods StableVITON Kim et al. (2023), OOTDiffusion Xu et al.
867 (2024), and IDM-VTON Choi et al. (2024). We directly utilize their open-sourced codes to generate
868 the try-on results. The qualitative comparison results are shown in the following figures. We see
869 that our method can generate human images with reference garments and maintain more details of
870 the garments than existing methods. For example, our method can preserve the texts and logos of
871 the reference garments well, while previous reference-net based methods OOTDiffusion and IDM-
872 VTON struggle to achieve this. We attribute the success to our strategy to extract the reference
873 features and synthesize target images using the same denoising network, eliminating the domain
874 gap between the reference and target images.

875 A.3 MORE VISUAL RESULTS ON CONSISTENT HUMAN IMAGE AND VIDEO GENERATION

876
877 **Failure cases.** As discussed in our main manuscript, our method may fail to generate consistent
878 images and videos in situations where the background is complex and the target pose significantly
879 deviates from the reference human image. As shown in Fig. 9, the complex background cannot be
880 maintained and some artifacts are brought to the foreground human. Furthermore, when the target
881 pose deviates considerably from the reference image, generating the unseen regions becomes chal-
882 lenging, leading to inconsistencies in the appearance of the human subject. To address these issues,
883 we plan to collect high-quality human videos that feature large motions and complex backgrounds.
884 This effort aims to enhance the model’s ability to handle diverse scenarios. Additionally, we will
885 explore more advanced base models to improve overall performance and robustness.

886 **Additional Visual Results.** We present additional animated videos featuring real human subjects
887 and cartoon characters in Fig.11 and the accompanying supplementary video. Our method demon-
888 strates highly competitive performance in animating both real-world individuals and cartoon charac-
889 ters. Furthermore, we can sequentially perform visual try-on and subsequently animate the generated
890 human, as illustrated in Fig.10.

891
892
893
894
895
896
897
898
899
900
901
902
903
904
905
906
907
908
909
910
911
912
913
914
915
916
917

918
 919
 920
 921
 922
 923
 924
 925
 926
 927
 928
 929
 930
 931
 932
 933
 934
 935
 936
 937
 938
 939
 940
 941
 942
 943
 944
 945
 946
 947
 948
 949
 950
 951
 952
 953
 954
 955
 956
 957
 958
 959
 960
 961
 962
 963
 964
 965
 966
 967
 968
 969
 970
 971

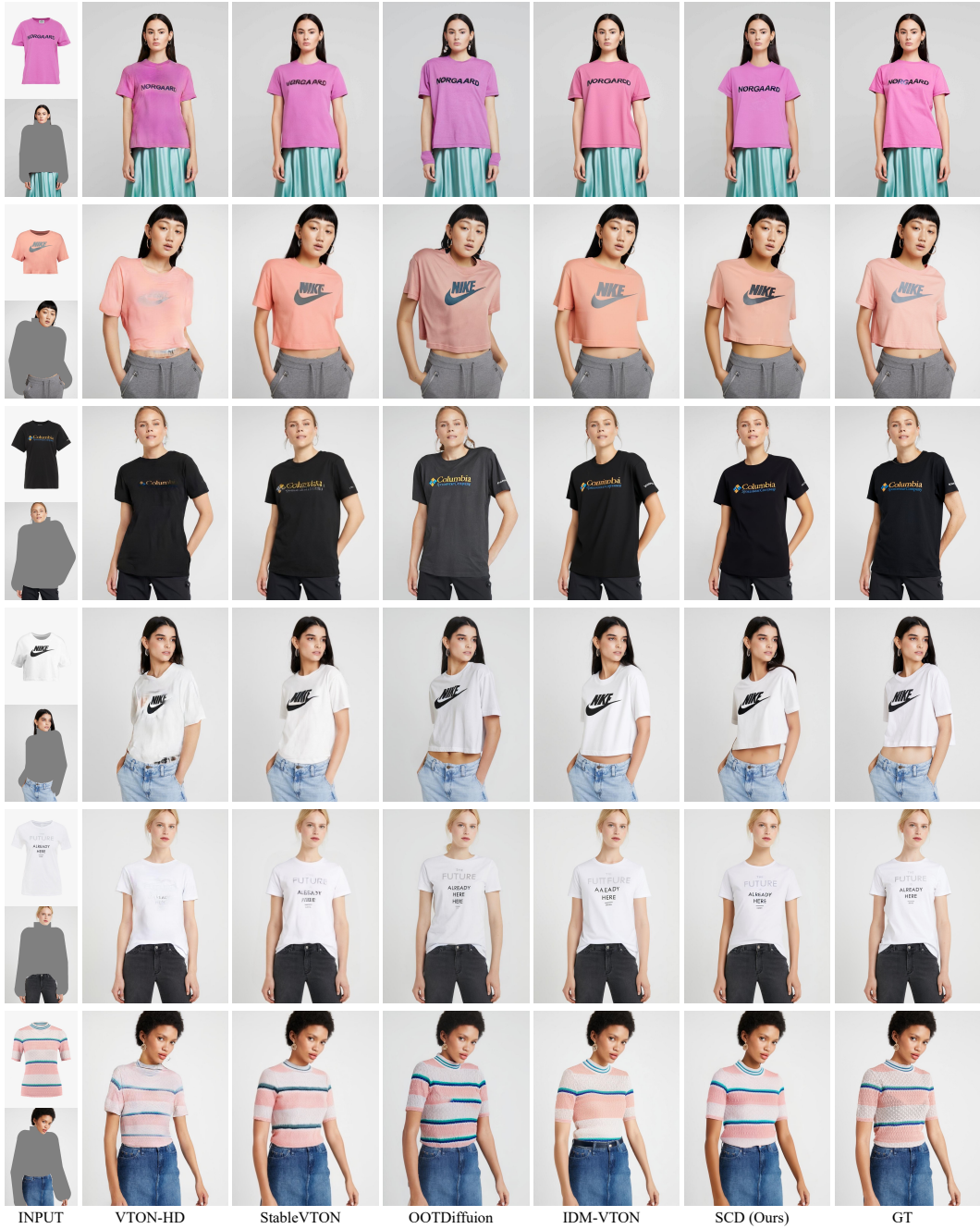


Figure 7: Qualitative comparison on the VITON-HD dataset (paired setting).

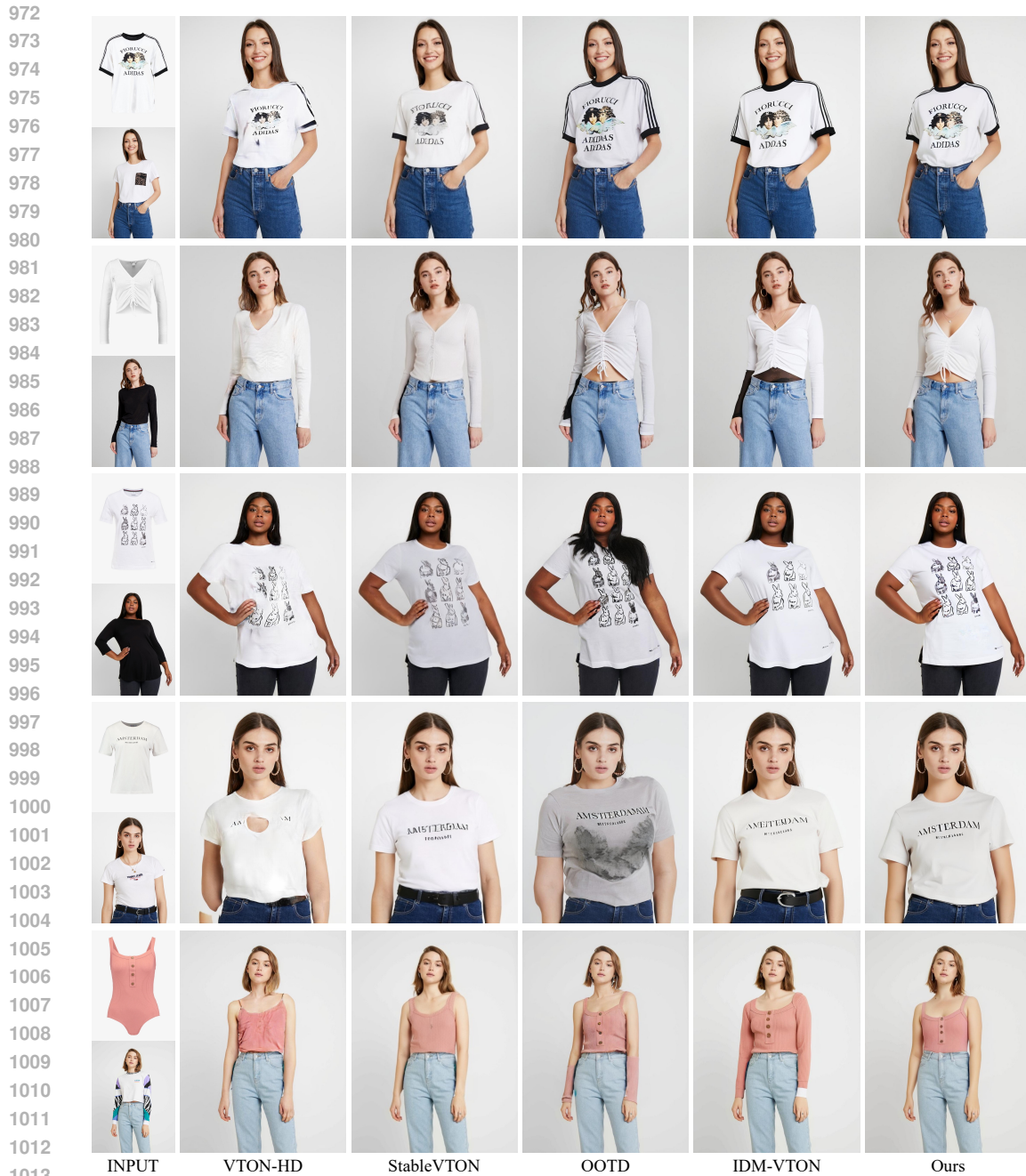


Figure 8: Qualitative comparison on the VITON-HD dataset (unpaired setting).

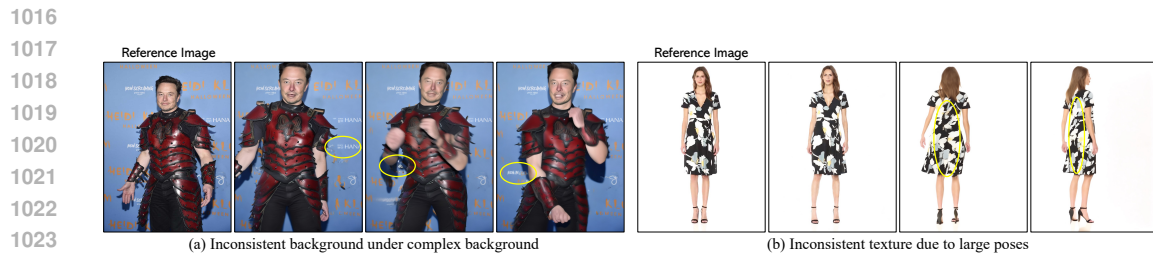


Figure 9: Failure cases under complex background and large poses.

1026
 1027
 1028
 1029
 1030
 1031
 1032
 1033
 1034
 1035
 1036
 1037
 1038
 1039
 1040
 1041
 1042
 1043
 1044
 1045
 1046
 1047
 1048
 1049
 1050
 1051
 1052
 1053
 1054
 1055
 1056
 1057
 1058
 1059
 1060
 1061
 1062
 1063
 1064
 1065
 1066
 1067
 1068
 1069
 1070
 1071
 1072
 1073
 1074
 1075
 1076
 1077
 1078
 1079



Figure 10: Results of sequentially performing try-on and animation.

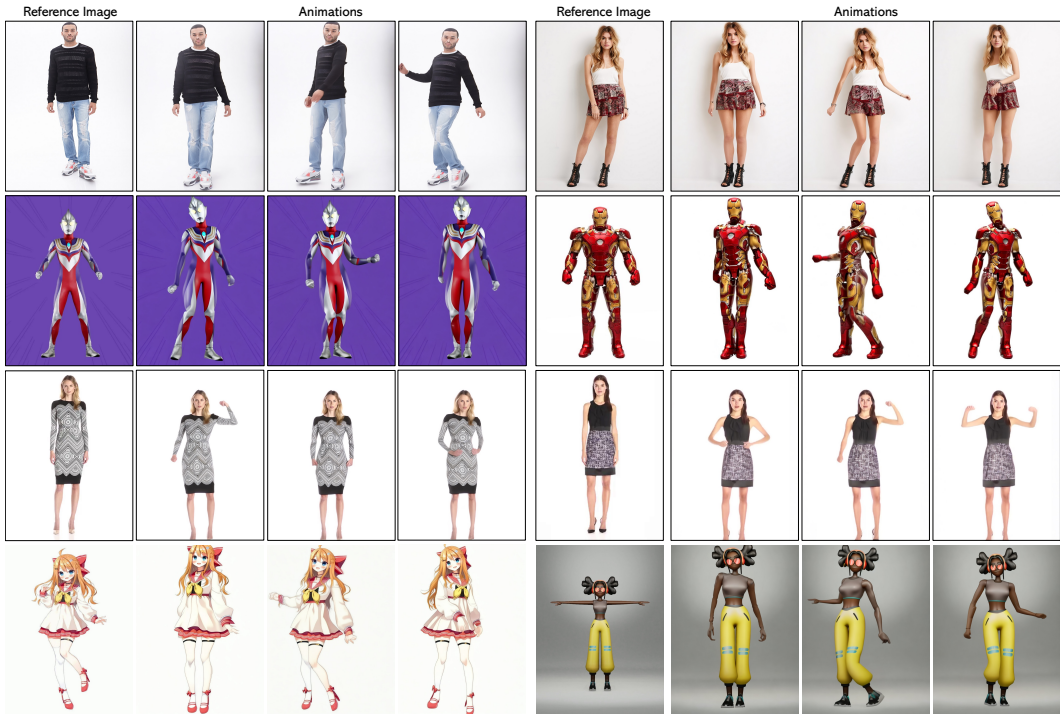


Figure 11: Animation results. Our method demonstrates highly competitive performance in animating real-world or cartoon characters.